HHS Public Access

Author manuscript

Pediatr Neurol. Author manuscript; available in PMC 2015 December 30.

Published in final edited form as:

Pediatr Neurol. 2014 November ; 51(5): 669–674.e5. doi:10.1016/j.pediatrneurol.2014.07.028.

Corpus Callosum Diffusion Tensor Imaging and Volume Measures Are Associated With Disease Severity in Pediatric Niemann-Pick Disease Type C1

Ryan Lee, MD[a,b,*], **Kalyna Apkarian, BS**[c], **Eun Sol Jung, MAc**[d], **Nicole Yanjanin, MSN**[e], **Shoko Yoshida, MD**[f], **Susumu Mori, PhD**[f], **Jina Park, BS**[g], **Andrea Gropman, MD**[h], **Eva H. Baker, MD, PhD**[i], and **Forbes D. Porter, MD, PhD**[e]

[a]Department of Neurology, Shriners Hospitals for Children—Honolulu, Honolulu, Hawaii [b]Department of Pediatrics, John A. Burns School of Medicine, University of Hawaii, Honolulu, Hawaii [c]Department of Biomedical Engineering, Whiting School of Engineering, The Johns Hopkins University, Baltimore, Maryland [d]Department of Psychiatry, Kennedy Krieger Institute, Baltimore, Maryland [e]Eunice Kennedy Shriver National Institute of Child Health and Human Development, National Institutes of Health, Bethesda, Maryland [f]Department of Radiology, Johns Hopkins University School of Medicine, Baltimore, Maryland [g]School of Medicine, New York University, New York, New York [h]Division of Neurogenetics, Children's National Medical Center, Washington DC [i]Department of Radiology and Imaging Sciences, National Institutes of Health, Bethesda, Maryland

Abstract

BACKGROUND—Niemann-Pick disease type C1 is a neurodegenerative lysosomal storage disorder. Without a highly effective treatment, biomarkers of severity would be beneficial for prognostication and testing new interventions. Diffusion tensor imaging has shown microstructural abnormalities in adults with Niemann-Pick disease type C1. This is the first study to apply diffusion tensor imaging and volume analysis to evaluate the corpus callosum in a pediatric and adolescent population of patients with Niemann-Pick disease type C1. We hypothesized that the callosal fractional anisotropy, volume, and cross-sectional area will negatively correlate with NPC severity score.

METHODS—Thirty-nine individuals with Niemann-Pick disease type C1 aged 1–21.9 years (mean = 11.1; S.D. = 6.1), and each received one magnetic resonance imaging examination. Severity score were obtained by examination and clinical observation. An atlas-based automated approach was used to measure fractional anisotropy, cross-sectional area, and volume. For comparative analysis and validation of this atlas-based approach, one midsagittal image was chosen and the corpus callosum manually traced to obtain cross-sectional area. Statistical analyses were applied to study the relationships between imaging and clinical severity.

[*]Communications should be addressed to: Dr. Lee; Shriners Hospitals for Children—Honolulu; 1310 Punahou Street; Honolulu, Hawaii 96826. rylee@shrinenet.org.

The authors report no conflicts of interest.

RESULTS—For patients with Niemann-Pick disease type C1, lower corpus callosum fractional anisotropy, volume, and cross-sectional area significantly correlate with higher severity score. Severity subdomain analysis revealed ambulation, speech, seizures, and incontinence have the strongest relationships with callosal measures. Comparison of atlas-based processing and manual tracing techniques demonstrated validity for the automated method.

CONCLUSIONS—For individuals with Niemann-Pick disease type C1, the corpus callosum measures correlate with clinical severity. These findings reveal promise for the discovery of new imaging biomarkers for this disorder.

Keywords

NPC; DTI; corpus callosum; volume; severity; Niemann-Pick; diffusion tensor

Introduction

Niemann-Pick disease type C (NPC) is an autosomal recessive neurodegenerative lysosomal storage disorder caused by a mutation of either *NPC1* or *NPC2*. Most NPC patients, about 95%, have mutations in the *NPC1* gene, and the remaining 5% have the mutations in the *NPC2* gene.[1,2] In patients with NPC1, cholesterol and glycosphingolipid metabolism is impaired in lysosomes.[1–3] The incidence of NPC is estimated as one in 120,000 live births.[1] NPC1 may manifest impairments throughout the lifespan but typically presents in childhood or adolescence. Common signs include hepatosplenomegaly, ataxia, vertical gaze palsy, and language impairment.[2] There is no highly effective treatment for NPC1; patients who have early onset of disease tend to progress at a more rapid rate leading to premature death.[2–4] Several biomarkers of NPC severity have already been established, including acidic compartment volume, cholesterol oxidation products, amyloid-β release, and the National Institutes of Health (NIH) severity scale.[7,27–30] Each of these markers has its advantages, but none of them directly measures injury to the central nervous system (CNS), a key site of end-organ damage in this disease. Therefore, we sought to evaluate the potential of diffusion tensor imaging (DTI) to serve as a biomarker for CNS damage in the pediatric NPC1 population.

There are a few published neuroimaging studies describing microstructural abnormalities in adult NPC patients through the use of DTI.[5,6] Corpus callosum (CC) measurements have been demonstrated to be significantly reduced in adult NPC, suggesting the CC as a marker of disease severity.[5,6] This study focuses on disease severity in the CC as measured by DTI and volume measurements in a large pediatric patient group. The aims of this study were to examine the relationship that patient NPC1 severity score has with callosal fractional anisotropy (FA), volume, and cross-sectional area. We hypothesize that these measures have a negative correlation with severity score.

Materials and Methods

Study population

This study was approved by the Institutional Review Board of the *Eunice Kennedy Shriver* National Institute of Child Health and Human Development in Bethesda, Maryland. Written

informed consent was obtained from parents or legal guardians and documented in the medical record. Assent was obtained when possible. This study involved 39 pediatric patients with a diagnosis of NPC1 based on clinical examination and biochemical or genetic testing. The diagnosis was confirmed by expert evaluators (N.Y. and F.D.P.).

Image acquisition and analysis

NPC1 subjects received one magnetic resonance imaging (MRI) examination on a Philips Achieva 3.0T magnetic resonance scanner. Scans were acquired from August 2006 through January 2012. Propofol was used for sedation on all subjects for the duration of each scan. Spatially matched axial magnetization-prepared rapid gradient-echo (MPRAGE), T_2-weighted imaging (T_2WI), and DTI sequences were obtained without gaps. Diffusion weighting was performed along 16 axes with a *b* value of 800 seconds/mm^2. DTI acquisition parameters included repetition time (TR), 6401 ms; echo time (TE), 60 ms; field of view (FOV), 224 × 224 mm; acquisition matrix, 112 × 112; reconstruction matrix, 128 × 128; in-plane resolution, 1.75 × 1.75 mm/pixel; acquisition duration, 2:27; slice thickness, 2 mm; and number of axial slices, 70. T_2WI acquisition parameters included TR, 5400 ms; TE, 100 ms; FOV, 220 × 165 mm; acquisition matrix, 384 × 227; reconstruction matrix, 512 × 512; in-plane resolution, 0.43 × 0.43 mm/pixel; acquisition duration, 2:25; slice thickness, 5 mm; and number of axial slices, 28.

The atlas-based segmentation of the CC was based on the three-dimensional T_1-weighted images, which uses a reference map rather than explicit anatomic landmarks. Parameters of patient scans before 2010 included axial MPRAGE; TE, 3.8 ms; TR, 8.2 ms; FA, 8°; FOV, 256 mm; acquisition matrix, 256 × 256; reconstruction matrix, 256 × 256; slice thickness, 1.0 mm; and number of excitations, 1. Parameters of patient scans after a scanner upgrade in 2010 included axial MPRAGE; TE, 6.5 ms; TR, 11.4 ms; FA, 6°; FOV, 220 mm; acquisition matrix, 256 × 131; reconstruction matrix, 256 × 256; slice thickness, 1.0 mm; and number of excitations, 2. Although there were hardware and software updates, the same *b* value was used so as not to affect the determination of FA. Volume was determined by counting the number of voxels in the original image that mapped into the atlas-defined structure.

In general, with shorter TE, the signal to noise ratio is expected to be higher because of T_2-relaxation decay. DTI is usually designed to achieve the shortest TE possible. The shortest TE is, in turn, determined by many imaging parameters such as the available gradient strength, gradient hardware performance, used pulse sequence, image matrix size, bandwidth, the skew rate, and parallel imaging factor. In our study, we shortened the TE by the minimization of the image matrix and using a relatively small *b* value. In addition, Philips scanners use the single spin-echo sequence, compared with the dual-echo sequence regularly used by Siemens and GE scanners, which also contributed to the shorter TE. A comprehensive analysis of the signal to noise ratio and bias using the similar image protocol has been published.[32]

All DTI data sets were processed offline using DTIStudio software (http://cmrm.med.jhmi.edu and http://www.MriStudio.org). The raw diffusion-weighted images were first coregistered to one of the $b = 0$ images using a 12-mode affine transformation of automated image registration.[20] The six elements of the diffusion tensor, the FA, and mean

diffusivity were calculated. The large deformation diffeomorphic metric mapping was performed to correct distortion caused by B_0 susceptibility according to a previous publication,[21] using T_2WI as the target and the $b = 0$ image as the DTI data. Then, after skull stripping, the images were first normalized to the JHU-DTI-MNI "Eve" template with a nine-parameter affine transformation of automated image registration. A nonlinear transformation, accomplished by dual-contrast large deformation diffeomorphic metric mapping, was applied,[22,23] using trace and FA images. The nonlinear image transformation and the atlas-based parcellation were performed using DiffeoMap and RoiEditor (http://cmrm.med.jhmi.edu and http://www.MriStudio.org).[24–26]

These procedures are reciprocal, so the inverse-transformed brain parcellation map was superimposed onto the original MRI images and led to parcellation of the brain into 130 anatomic structures.[24–26] When the quantitative values were obtained, the cerebrospinal fluid spaces were excluded by a mean diffusivity threshold set at 0.0020 mm^2/second. This parcellation determined CC FA, volume, and cross-sectional area for each patient. Additionally, it enabled segmentation of the CC into six regions by defining right and left halves of the CC relative to the midline: left genu, right genu, left body, right body, left splenium, and right splenium. FA and volume were determined for each region. Then, as a gold-standard verification of the atlas-based method described previously, comparative analysis of cross-sectional area was performed using manual tracing of the CC on a single midsagittal image. FA and cross-sectional area measures of the manual tracing were then analyzed in comparison with the automated method.

Severity score, DTI, and volume measurements

The NIH NPC neurological severity score was developed to enable clinicians to derive a measure of severity based on history, observation, and physical examination.[7] Scores increase with disease severity. There are 17 subcategories that are summed to derive a total severity score: eye movement, ambulation, speech, swallowing, motor, cognition, hearing, memory, seizures, cataplexy, narcolepsy, behavior, psychology, hyperreflexia, incontinence, respiratory, and auditory brainstem response. The NIH NPC neurological severity score allows the assessment of clinical severity independent of age of disease onset, allowing the same scoring system to be used on children and adolescents.[7] The subscores, in addition to the age at first symptoms, duration of symptoms, and the presence of CoQ10 and miglustat therapies, were analyzed with DTI and volume measurements. Analysis of covariance was used for statistical analysis of all data except CoQ10 and miglustat therapy, with age at scan as a covariate. A Mann-Whitney nonparametric *t* test was used to analyze the presence of CoQ10 and miglustat therapies with DTI and volumetric measurements. For all statistical analyses, a *P* value less than 0.05 was chosen as the threshold of statistical significance.

Results

Patient population and demographics

We studied 39 patients with NPC1 (20 female and 19 male patients) between the ages of 1 and 21.9 years (mean = 11.1; S.D. = 6.1). The ethnic and racial distribution of patients was Caucasian (87%), Hispanic (12%), and American Indian (1%). The most common

presenting signs were splenomegaly or hepatomegaly, jaundice, and vertical gaze palsy. NIH neurological severity scores of this NPC1 population ranged from 1 to 46 points (mean = 16.2; S.D. = 11.5). The age of first symptoms ranged from birth to 13 years (mean = 2.7 years; S.D. = 3.6). The average duration of neurological symptoms at the time of scan was 7 years (S.D. = 4.1). At the time of the MRI examination, 21 subjects were receiving off-label oral miglustat as medical therapy and 26 subjects were receiving CoQ10 supplementation. Table 1 provides additional detailed data.

Whole corpus callosum, automated measures

For patients with NPC1, high NIH neurological severity score strongly correlated with low FA and low volume in the automated atlas-based approach (Table 2). The total severity score demonstrated a strong negative correlation with automated whole CC FA and whole CC volume. The FA and volume of segmented CC regions revealed similarly strong negative correlations with the total severity score. Figure 1 illustrates a plot of whole CC FA versus NIH neurological severity score, demonstrating a strong negative correlation with an R^2 value of 0.37. Figure 2 illustrates a similar negative correlation of whole CC volume versus NIH neurological severity score with an R^2 value of 0.22.

Automated whole CC FA and volume were correlated with NIH neurological severity score subcategories. Supplementary Table 1 describes the statistically significant correlations. The ambulation, speech, swallow, motor, cognition, memory, seizures, and incontinence subscores all revealed a strong negative correlation with both the automated whole CC FA and volume. The eye movement sub-score revealed a weak negative correlation with the automated whole CC FA. These weak negative correlations were present in all CC regions except the right genu. Eye movement demonstrated a negative correlation with the automated whole CC volume in all regions except for the genu and the left splenium. The narcolepsy subscore revealed a negative correlation with automated whole CC FA in all regions except the splenium. It did not correlate with automated whole CC volume measurements, except for the left genu. The hyperreflexia subscore followed a similar pattern revealing weak correlation with automated whole CC FA in all regions except the splenium. There was a negative correlation between hyperreflexia and automated whole CC volume. The presence of CoQ10 therapy only reached statistical significance in one region, the left and right body of the CC. Hearing, cataplexy, behavior, psychology, respiratory, and auditory brainstem response subscores did not correlate with DTI and volume measurements. Similarly, the age at first symptoms, the duration of neurological symptoms, and the presence of miglustat therapy did not correlate with DTI measures. Supplementary Tables 2 and 3 describe the statistically nonsignificant correlations.

Midsagittal slice, manual measures

For patients with NPC1, high NIH neurological severity score strongly correlated with low FA and low cross-sectional area in the manual tracing of the midsagittal slice (Table 2). The total severity score demonstrated a strong negative correlation with the manual midsagittal FA and cross-sectional area.

Manual midsagittal FA and cross-sectional area were correlated with NIH neurological severity score subcategories (Supplementary Table 1). The ambulation, speech, swallow, motor, cognition, memory, seizures, and incontinence subscores all revealed a strong negative correlation with both the midsagittal FA and cross-sectional area. The eye movement subscore correlated with midsagittal FA but not with cross-sectional area. The narcolepsy subscore did not correlate with midsagittal FA or volume. Similarly, the hyperreflexia subscore did not correlate with midsagittal FA or volume. Hearing, cataplexy, behavior, psychology, respiratory, and auditory brainstem response subscores did not correlate with DTI and volume measurements. Similarly, the age at first symptoms, the duration of symptoms, and the presence of CoQ10 and miglustat therapies did not reach statistical significance in this region (Supplementary Tables 2 and 3).

Midsagittal slice, automated measures

For patients with NPC1, high NIH neurological severity score strongly correlated with low FA and low cross-sectional area in the automated tracing of the midsagittal slice (Table 2). The total severity score demonstrated a strong negative correlation with the automated midsagittal FA and cross-sectional area.

Automated midsagittal FA and cross-sectional area were correlated with NIH neurological severity score subcategories (Supplementary Table 1). The ambulation, speech, swallow, motor, cognition, memory, seizures, and incontinence subscores all revealed a strong negative correlation with both midsagittal FA and cross-sectional area. The eye movement subscore did not correlate with midsagittal FA or cross-sectional area. The narcolepsy subscore weakly correlated with midsagittal FA but not with volume. Similarly, the hyperreflexia subscore weakly correlated with the automated midsagittal FA but not with volume. The hearing, cataplexy, behavior, psychology, respiratory, and auditory brainstem response subscores did not correlate with DTI and volume measurements. Similarly, the age at first symptoms, the duration of symptoms, and the presence of CoQ10 and miglustat therapies did not reach statistical significance in this region (Supplementary Tables 2 and 3).

Additionally, the agreement between these automated and manual methods is validation for the atlas-based approach detailed previously. The correlations between the total NIH neurological severity score and both FA and cross-sectional area in the whole CC were significant ($P < 0.01$) in both the automated atlas-based and manual methods. Supplementary Tables 1–3 demonstrate this validation.

Discussion

For NPC1 patients in our study, a high NIH neurological severity score was associated with low callosal FA, low CC segmental volume, and low total CC cross-sectional area. Although all the components of the NIH neurological severity score are important, the ambulation and motor function domains reveal the strongest correlation with disease severity and should be noted as such for future clinical studies. These findings support our hypothesis that there is a negative relationship between DTI measures, specifically, microstructural impairment of the CC, and the clinical severity in pediatric patients with NPC1.

Consistent with our findings, previous studies and case reports using DTI demonstrate architectural differences in white matter in individuals with NPC, and case reports suggest a similar pattern.[6,8] Collectively, our findings of volume reduction and decreased FA in the CC, along with increasing clinical severity suggest that neurobiologic pathology can be measured In Vivo. Studies involving amyloid-β protein and cholesterol accumulation are at the forefront of hypotheses investigating neurodegeneration in NPC1.[9–11] Current therapeutic intervention for NPC includes miglustat, an iminosugar that has been reported to provide modest benefit for NPC1 patients by reversibly inhibiting the synthesis of glucosylceramides.[31] This is intended to prevent the production, and thus accumulation, of glycosphingolipids in patients with lysosomal storage disorders, resulting in the stabilization of a few signs such as tremor, dysarthria, cataplexy, and eye movement in juvenile-onset patients.[4,12–14] Although miglustat reveals a potential benefit for slowing disease progression, our findings do not demonstrate a correlation between miglustat therapy and structural neuroimaging measurements. This lack of significance may be because of a small effect of the drug not detectable in our sample and the power of our test. It may also be because of our pediatric group representing a population sample with increased severity, which is more consistent with pediatric-onset NPC.[4,12,13] Interestingly, several lines of evidence demonstrate 2-hydroxypropyl-beta-cyclodextrin that facilitates the efflux of unesterified cholesterol from the late endosome and/or lysosome in NPC1 models.[15–19] This represents a promising area of the future study.

A potential limitation of this study is the absence of control subjects. The aim of this study was to examine the relationship between DTI measures and disease severity among the NPC1 population, and this was accomplished through a noncontrol study. Although FA and volume of the CC varies with age and gender, we were unable to recruit matched controls. At the time of this study, no control data is publicly available that was acquired under similar imaging parameters. Therefore, our findings of a relationship between CC and clinical severity demonstrate correlation as group data, and further studies determining this variance among age and gender matched controls are needed.

Our findings suggest that callosal measurements are a promising area requiring further research. Although this study suggests the benefits that an imaging biomarker may provide based on a patient's single scan, assessing the progression of the disease through microstructural analysis is the next step. These data show promise, but larger longitudinal studies in humans are required to determine the benefit of medical therapy on long-term neuro-developmental disability. Based on the previously mentioned results, imaging may play an important role in determining the efficacy of any such therapy. Additionally, the reliability of an automated method was validated with manual tracing.

Conclusions

DTI and volume measurements of the CC are associated with disease severity in pediatric and young adult patients with NPC1. Future studies applying brain microstructural analysis to longitudinal functional and behavioral outcomes will improve our understanding of NPC1, in addition to providing a biomarker of CNS damage and disease severity that can be used for the evaluation of future interventions.

Supplementary Material

Refer to Web version on PubMed Central for supplementary material.

Acknowledgments

This work was supported by the intramural research program of the *Eunice Kennedy Shriver* National Institute of Child Health and Human Development, National Institutes of Health (NIH). The authors thank the magnetic resonance imaging technologists who acquired the images for this project (Mastaneh Owhadi RT, Bonita Damaska RT, and Betty Wise RT). The authors express their appreciation to the families and patients who participated in these studies. This article was supported by a Bench to Bedside award from the NIH Clinical Center and Office of Rare Diseases. This article was supported by the Ara Parseghian Medical Research Foundation.

References

1. Vanier MT. Niemann-Pick disease type C. Orphanet J Rare Dis. 2010; 5:16. [PubMed: 20525256]
2. Patterson MC, Hendriksz CJ, Walterfang M, et al. Recommendations for the diagnosis and management of Niemann-Pick disease type C: an update. Mol Genet Metab. 2012; 106:330–344. [PubMed: 22572546]
3. Lossos A, Schlesinger I, Okon E, et al. Adult-onset Niemann-Pick type C disease. Clinical, biochemical, and genetic study. Arch Neurol. 1997; 54:1536–1541. [PubMed: 9400363]
4. Paciorkowski AR, Westwell M, Ounpuu S, et al. Motion analysis of a child with Niemann-Pick disease type C treated with miglustat. Mov Disord. 2008; 23:124–128. [PubMed: 17973331]
5. Walterfang M, Fahey M, Abel L, et al. Size and shape of the corpus callosum in adult Niemann-Pick type C reflects state and trait illness variables. AJNR Am J Neuroradiol. 2011; 32:1340–1346. [PubMed: 21596811]
6. Trouard TP, Heidenreich RA, Seeger JF, Erickson RP. Diffusion tensor imaging in Niemann-Pick type C disease. Pediatr Neurol. 2005; 33:325–330. [PubMed: 16243219]
7. Yanjanin NM, Velez JI, Gropman A, et al. Linear clinical progression, independent of age of onset, in Niemann-Pick disease, type C. Am J Med Genet B Neuropsychiatr Genet. 2010; 153B:132–140. [PubMed: 19415691]
8. Walterfang M, Fahey M, Desmond P, et al. White and gray matter alterations in adults with Niemann-Pick disease type C: a cross-sectional study. Neurol. 2010; 75:49–56.
9. Vincent I, Bu B, Erickson RP. Understanding Niemann-Pick type C disease: a fat problem. Curr Opin Neurol. 2003; 16:155–161. [PubMed: 12644742]
10. Saito Y, Suzuki K, Nanba E, Yamamoto T, Ohno K, Murayama S. Niemann-Pick type C disease: accelerated neurofibrillary tangle formation and amyloid beta deposition associated with apolipoprotein E epsilon 4 homozygosity. Ann Neurol. 2002; 52:351–355. [PubMed: 12205649]
11. Yamazaki T, Chang TY, Haass C, Ihara Y. Accumulation and aggregation of amyloid beta-protein in late endosomes of Niemann-pick type C cells. J Biol Chem. 2001; 276:4454–4460. [PubMed: 11085995]
12. Perez-Poyato MS, Pineda M. New agents and approaches to treatment in Niemann-Pick type C disease. Curr Pharm Biotechnol. 2011; 12:897–901. [PubMed: 21235443]
13. Zarowski M, Steinborn B, Gurda B, Dvorakova L, Vlaskova H, Kothare SV. Treatment of cataplexy in Niemann-Pick disease type C with the use of miglustat. Eur J Paediatr Neurol. 2011; 15:84–87. [PubMed: 20207562]
14. Scheel M, Abegg M, Lanyon LJ, Mattman A, Barton JJ. Eye movement and diffusion tensor imaging analysis of treatment effects in a Niemann-Pick type C patient. Mol Genet Metab. 2010; 99:291–295. [PubMed: 19939718]
15. Ward S, O'Donnell P, Fernandez S, Vite CH. 2-hydroxypropyl-beta-cyclodextrin raises hearing threshold in normal cats and in cats with Niemann-Pick type C disease. Pediatr Res. 2010; 68:52–56. [PubMed: 20357695]
16. Matsuo M, Togawa M, Hirabaru K, et al. Effects of cyclodextrin in two patients with Niemann-Pick type C disease. Mol Genet Metab. 2013; 108:76–81. [PubMed: 23218948]

17. Wehrmann ZT, Hulett TW, Huegel KL, et al. Quantitative comparison of the efficacy of various compounds in lowering intracellular cholesterol levels in Niemann-Pick type C fibroblasts. PLoS One. 2012; 7:e48561. [PubMed: 23144769]
18. Maulik M, Ghoshal B, Kim J, et al. Mutant human APP exacerbates pathology in a mouse model of NPC and its reversal by a beta-cyclodextrin. Hum Mol Genet. 2012; 21:4857–4875. [PubMed: 22869680]
19. Taylor AM, Liu B, Mari Y, Liu B, Repa JJ. Cyclodextrin mediates rapid changes in lipid balance in Npc1−/− mice without carrying cholesterol through the bloodstream. J Lipid Res. 2012; 53:2331–2342. [PubMed: 22892156]
20. Woods RP, Grafton ST, Holmes CJ, et al. Automated image registration: I. General methods and intrasubject, intramodality validation. J Comp Assist Tomogr. 1998; 22:139–152.
21. Huang H, Ceritoglu C, Li X, et al. Correction of B0 susceptibility induced distortion in diffusion-weighted images using large-deformation diffeomorphic metric mapping. Magn Reson Imaging. 2008; 26:1294–1302. [PubMed: 18499384]
22. Miller MI, Beg MF, Ceritoglu C, Stark C. Increasing the power of functional maps of the medial temporal lobe by using large deformation diffeomorphic metric mapping. Proc Natl Acad Sci U S A. 2005; 102:9685–9690. [PubMed: 15980148]
23. Beg MF, Miller MI, Trouve A, Younes L. Computing large deformation metric mappings via geodesic flows of diffeomorphisms. Int J Comput Vis. 2005; 61:139–157.
24. Oishi K, Faria A, Jiang H, et al. Atlas-based whole brain white matter analysis using large deformation diffeomorphic metric mapping: application to normal elderly and Alzheimer's disease participants. Neuroimage. 2009; 46:486–499. [PubMed: 19385016]
25. Faria AV, Zhang J, Oishi K, et al. Atlas-based analysis of neuro-development from infancy to adult hood using diffusion tensor imaging and applications for automated abnormality detection. Neuroimage. 2010; 52:415–428. [PubMed: 20420929]
26. Faria AV, Hoon AH Jr, Stashinko EE, et al. Quantitative analysis of brain pathology based on MRI and brain atlases–applications for cerebral palsy. Neuroimage. 2011; 54:1854–1861. [PubMed: 20920589]
27. te Vruchte D, Speak AO, Wallom KL, et al. Relative acidic compartment volume as a lysosomal storage disorder–associated biomarker. J Clin Invest. 2014; 124:1320–1328. [PubMed: 24487591]
28. Porter FD, Scherrer DE, Lanier MH, et al. Cholesterol oxidation products are sensitive and specific blood-based biomarkers for Niemann-Pick C1 disease. Sci Transl Med. 2010; 2:56–81.
29. Mattsson N, Zetterberg H, Bianconi S, et al. γ-Secretase-dependent amyloid-β is increased in Niemann-Pick type C. Neurology. 2010; 76:366–372. [PubMed: 21205675]
30. Cluzeau CVM, Watkins-Chow DE, Fu R, et al. Microarray expression analysis and identification of serum biomarkers for Niemann–Pick disease, type C1. Hum Mol Genet. 2012; 21:3632–3646. [PubMed: 22619379]
31. Patterson MC, Vecchio D, Prady H, Abel L, Wraith JE. Miglustat for treatment of Niemann-Pick C disease: a randomised controlled study. Lancet Neurol. 2007; 6:765–772. [PubMed: 17689147]
32. Landman BA, Farrell JA, Jones CK, Smith SA, Prince JL, Mori S. Effects of diffusion weighting schemes on the reproducibility of DTI-derived fractional anisotropy, mean diffusivity, and principal eigenvector measurements at 1.5T. Neuroimage. 2007; 36:1123–1138. [PubMed: 17532649]

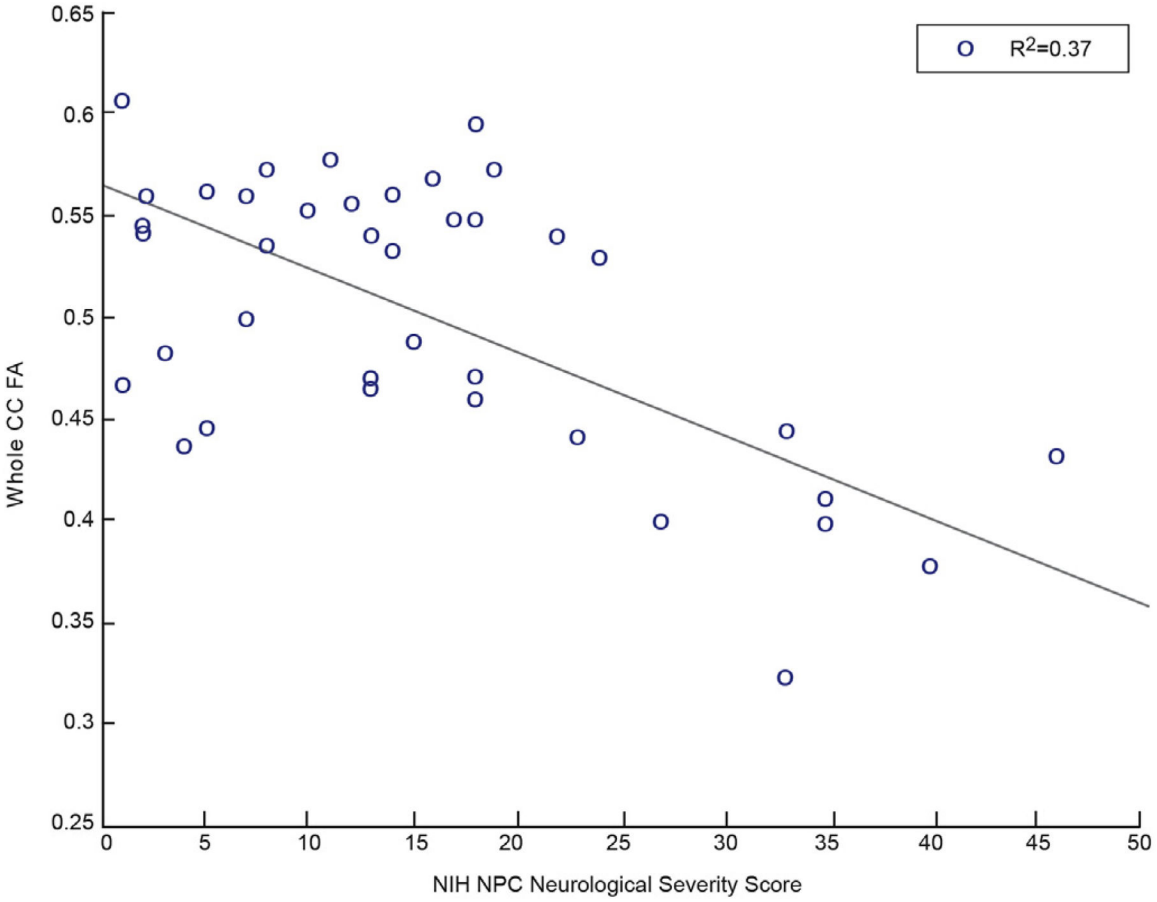

FIGURE 1.

Whole CC FA shows significant negative correlation with NPC severity score. (Color version of this figure is available in the online edition.)

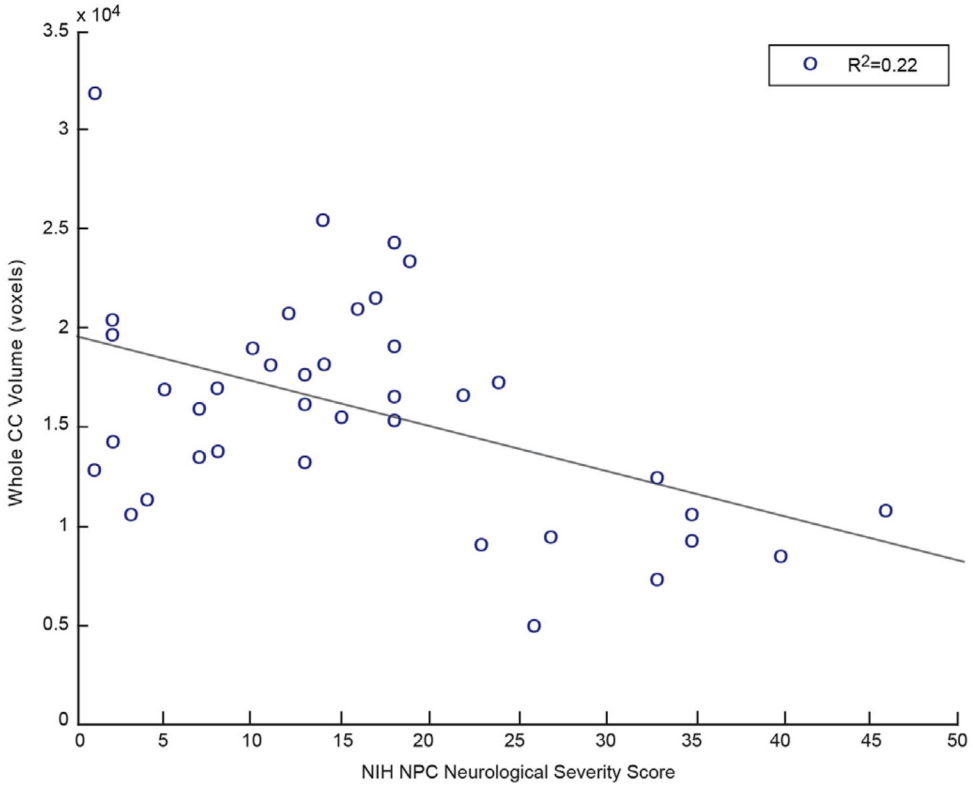

FIGURE 2.

Whole CC volume shows significant negative correlation with NPC severity score. (Color version of this figure is available in the online edition.)

TABLE 1

Detailed Demographic and Clinical Data for Niemann-Pick Disease Type C Patients (n = 39)

Patient	Sex	Age	Total SS	Presenting Symptom	Age at First Symptom (mo)	Duration of Neurological Symptoms (yr)	Miglustat (+/−)	CoQ10 (+/−)
1	F	21.2	35	Splenomegaly	18	12.2	−	+
2	M	7.7	5	Splenomegaly	6	2.7	+	+
3	F	13.1	33	Splenomegaly	8	11.1	+	−
4	M	5	11	Jaundice, splenomegaly	0	2.0	−	−
5	M	10	14	Splenomegaly	12	7.0	−	+
6	M	16.3	18	Hepatosplenomegaly	18	13.3	−	+
7	F	11.8	22	Splenomegaly	2	10.3	−	+
8	F	4	26	Splenomegaly	6	2.0	+	+
9	M	7.7	7	Jaundice, Splenomegaly	0.5	5.7	+	+
10	M	11.8	18	Splenomegaly	18	5.8	+	+
11	M	5.4	8	Hepatosplenomegaly	3	3.4	+	+
12	F	5.2	13	Hepatosplenomegaly	0	4.2	+	+
13	M	4.7	2	Jaundice, splenomegaly	0	Unknown	+	+
14	M	6.1	7	Hepatosplenomegaly, jaundice	0.75	4.1	−	+
15	F	3.8	3	Splenomegaly	24	1.7	−	+
16	F	21.5	35	Vertical gaze palsy	60	16.5	−	+
17	F	6.7	40	Fine motor ataxia	36	3.7	−	+
18	F	15.7	1	Splenomegaly	24	Unknown	+	+
19	F	6.8	27	Fetal ascites	0	5.3	+	+
20	F	12.6	24	Developmental delay	60	7.6	−	+
21	F	16.8	23	Learning delay	Unknown	8.8	+	+
22	M	8.4	46	Clumsy	18	6.9	−	+
23	M	1	1	Jaundice	0	Unknown	+	+
24	M	1.6	4	Jaundice	1.25	Unknown	−	+
25	M	17.2	10	Unsteady gait	144	5.2	+	+
26	F	8.1	8	Splenomegaly	15	1.1	+	+
27	M	20.3	14	Cognitive decline, slurred speech	156	7.3	−	+
28	M	6.6	13	Fetal ascites	0	3.1	−	+

Patient	Sex	Age	Total SS	Presenting Symptom	Age at First Symptom (mo)	Duration of Neurological Symptoms (yr)	Miglustat (+/−)	CoQ10 (+/−)
29	M	4	2	Jaundice, HSM	0	Unknown	−	−
30	F	12.7	17	Learning disability	96	4.7	+	−
31	F	21	18	Hepatosplenomegaly	48	16.0	−	−
32	F	15.6	12	Fetal ascites	0	Unknown	+	−
33	M	17.2	19	Nonverbal learning disability	72	11.2	−	−
34	F	21.9	18	Learning difficulty	132	10.9	−	−
35	F	17.3	15	Clumsy	84	10.2	+	−
36	F	13.3	13	Learning disability	84	6.3	+	−
37	M	15.2	33	Seizures	72	9.2	+	−
38	F	11.8	16	Hepatosplenomegaly	7	8.7	+	−
39	M	3.8	2	Splenomegaly	6	1.7	+	−

Abbreviations:

F = Female

HSM = hepatosplenomegaly

M = Male

SS = National Institutes of Health Niemann-Pick disease type C neurological severity score

Duration of neurological symptoms is “unknown” when presenting symptom reported was not neurological, and onset of neurological symptom was not reported.

Pediatr Neurol. Author manuscript; available in PMC 2015 December 30.

TABLE 2

Total National Institutes of Health Niemann-Pick Disease Type C Neurological Severity Score Correlations

Measure	Location	*P*	*r*	*F*
FA	L genu	<0.01	−0.69	34.43
	L body	<0.01	−0.66	28.85
	L splenium	<0.01	−0.56	16.55
	R genu	<0.01	−0.54	14.84
	R body	<0.01	−0.73	41.38
	R splenium	<0.01	−0.56	16.84
	Total	<0.01	−0.66	29.25
Volume	L genu	<0.01	−0.55	16.7
	L body	<0.01	−0.61	24.45
	L splenium	<0.01	−0.57	18.91
	R genu	<0.01	−0.55	16.38
	R body	<0.01	−0.65	29.5
	R splenium	<0.01	−0.54	16.6
	Total	<0.01	−0.6	21.94
Manual midsagittal				
FA	Midsagittal	<0.01	−0.64	26.3
CC cross-sectional area	Midsagittal	<0.01	−0.64	25.29
Automated midsagittal				
FA	Midsagittal	<0.01	−0.64	26.1
CC cross-sectional area	Midsagittal	<0.01	−0.44	10.12

Abbreviations:

CC = Corpus callosum

F = Variance ratio

FA = Fractional Anisotropy

L = Left

r = Correlation coefficient

R = Right